Super resolution for fundoscopy based on 3D image registration

Carlos Hernandez-Matas[1] and Xenophon Zabulis[2]

Abstract— **An approach to the generation of super-resolution (SR) images from fundoscopy images is proposed that is based on the 3D registration of the original fundoscopy images. The proposed approach utilizes a simple 3D registration method to enable the application of conventional SR techniques which, otherwise, employ 2D image registration. Qualitative and quantitative comparative evaluation shows that the obtained results improve image definition and alleviate noise.**

I. INTRODUCTION

Small vessel structure and function assessment can lead to more accurate and timely diagnosis, whose common denominator is vasculopathy i.e. hypertension, diabetes and a number of autoimmune disorders [1]. Due to their minute scale, small vessels are more sensitive to diseases that affect the cardiovascular system. For this reason, the damage on small vessels starts much earlier and, thus, its timely detection is of diagnostic significance.

Small vessels are spread throughout the body, located in all internal and external organs. Of them, the retina provides an open and accessible window for assessing their condition. Retinal small vessels can be imaged through fundoscopy, a cost and time efficient and, most importantly, non-invasive technique which is thereby suitable for screening. During the fundoscopy examination, or more precisely fundus photography, the subject rests his/her head on a chin rest. Thereby, images acquired from the same eye are coarsely aligned due to the approximately same accommodation of the eye relative to the imaging sensor.

Examinations of vasculature condition involve the measurement of vessel widths and, in particular, the relationship between arterial and venular widths; a widely employed pertinent metric is the Arteriolar-to-Venular diameter Ratio (AVR) [2]. Improvement of the resolution and definition by which retinal vessels are imaged is thus of interest because, this way, pertinent diagnostic metrics can be more accurately computed.

Super Resolution (SR) methods utilize multiple images of the same scene acquired from slightly different viewpoints to provide an image of higher resolution and definition; in fundoscopy, imaging of the retina from slightly different perspectives is inherent due to saccadic motion. The basis of SR methods is image registration, because it enables the utilization of pixels from different images to be considered as additional samplings of the same function. Most SR methods treat the problem of combining multiple images in a 2D context [3], [4], [5]. This has been also the case in the application of SR methods in retinal images [6], [7]. That is, the underlying registration method considers only 2D translation and rotation, assuming that perspective differences across images are negligible. Although that there exist retinal image registration methods which account for the 3D geometry of the retinal surface [8], [9], [10], [11], [12], [13], [14], [15], to the best of our knowledge, they have not been employed in the problem of SR. Not related to retinal imaging, the work in [16] considers surface orientation and camera pose but only for 3D surface patches rather than entire surfaces.

In this work, we suggest that by considering perspective differences and without requiring camera calibration, better SR images can be obtained by conventional SR methods. As an initial step, we approximate the retinal region of interest to be planar and thereby use a homography as a basis for 3D image registration. Indeed, the retina is not a planar surface however the region of interest for computing the metrics such as the AVR is limited to 10-15 degrees of visual angle where the planarity assumption is sufficient. We acknowledge that accounting for the 3D structure of the retina would lead to even better image registration and, in turn, SR images; we regard this as a next future step of this work. However, as discussed in Sec. IV solving for the 3D eye structure would additionally require camera calibration. Our argument is that since we can obtain better SR images with homography-based 3D registration, as opposed to existing SR methods that perform 2D image registration, results would only improve if 3D registration is further improved by solving for the 3D structure of the eye and the camera parameters.

II. METHOD

The proposed method operates on a set of images, of the same eye. One of these images is selected as the *reference*. Assuming that approximately the same eye region appears in all of them, currently this selection is arbitrary, i.e. the first. Typically, color images are available, from which only the "green" channel is utilized, being the one offering a higher contrast in fundoscopy [17].

Keypoint features are detected in all images and matched with those found in the reference image establishing potential correspondences. Several keypoint descriptors, including SIFT [18] were evaluated for the task using their OpenCV

This research was made possible by a Marie Curie grant from the European Commission in the framework of the REVAMMAD ITN (Initial Training Research network), Project number 316990.

[1]C. Hernandez-Matas is with Institute of Computer Science, Foundation for Research and Technology – Hellas, Heraklion, GR-70013, Greece and Computer Science Department, University of Crete, Heraklion, GR-70013, Greece. carlos at ics.forth.gr

[2]X. Zabulis is with Institute of Computer Science, Foundation for Research and Technology – Hellas, Heraklion, GR-70013, Greece. zabulis at ics.forth.gr

978-1-4244-7929-0/14/$26.00 ©2014 IEEE

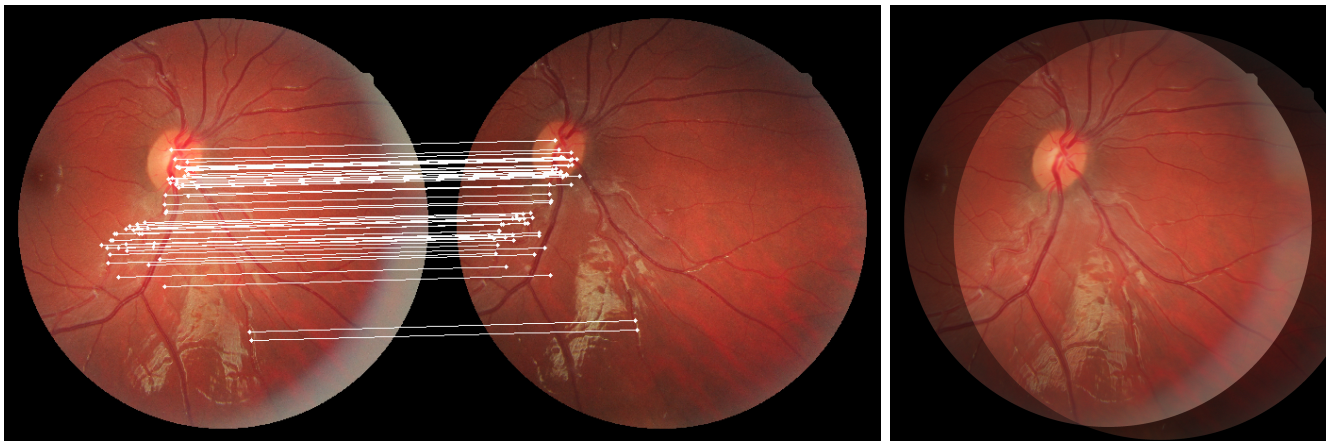

Fig. 1. Registration of retinal images. Keypoint matches (left, middle) and superimposition of the registered images (right).

implementations[1]. In accordance to findings in the literature [19], [20] and to our own observations, we selected SURF [21] mainly due to their improved robustness to spurious matches, as well as their localization accuracy. In addition, though SIFT features are reported to be more in generic datasets [22], in our case we found that the amount of keypoints found by SURF in retinal images is larger. Matching is performed conventionally as in [18], requiring a high (> 0.8) Nearest Neighbor Distance Ratio to establish a match. Input images are coarsely aligned due to the accommodation of the subject's head with the modality's chin rest (see Sec. I). Thereby, a preliminary spurious-match rejection is simple to achieve based on the relative locations of keypoints that are considered for matching, without risking the omission of a correct match. This rejection facilitates the robustness of the next step of the proposed method, as it simplifies the robust estimation of the pursued homography.

A homography H_i is established between the reference image and each image i in the set. A homography is a perspective transformation between two planes and is represented by a 3×3 matrix H. A homogeneous 2D point upon the first plane, let $\mathbf{x} = [x\ y\ 1]^T$ is transformed to occur at its corresponding location on the second plane as $H \cdot \mathbf{x}$, where $\cdot$ denotes matrix multiplication. In our case, the two planes are the reference and the image to be registered. For the reference image $i = 0$, H_0 is the identity matrix.

Each homography H_i is estimated robustly to eliminate remaining false matches. A RANSAC [23] process is employed for this purpose and the final result is availed by least-squares fitting of the homography to the inliers of the consensus. The least squares solution is found by application of the Levenberg-Marquardt algorithm [24].

Based on the estimated homography H_i, image i is warped to be registered to the reference image, as follows. For each point $\mathbf{x}$ of the reference image, its corresponding point in the registered image is $\mathbf{x}' = H^{-1} \cdot \mathbf{x}$. As point $\mathbf{x}'$ typically occurs at non-integer coordinates, its intensity value is found by bicubic interpolation of the original image registered to the reference one. The operation is demonstrated in Fig. 1.

The general model of the SR problem states that a given image captured by a device, is a noisy, blurred and downsampled representation of a scene. Via a combination of multiple images of the same scene, a closer version of the scene can be reconstructed in a SR image [25]. The prerequisite for such an operation is a registration mapping across the input images, in order for the multiple samples to be spatially combined. The resulting image is provided at a higher resolution than the original. The increment in resolution is called the scaling factor. It is worth noting that if the scaling factor is n, and l is the number of images, if $l < n^2$ the problem is undetermined, if $l = n^2$ it is a square problem, and if $l > n^2$ the problem is overdetermined [26].

Once the registration between the reference and the rest of the images has been determined, conventional SR methods can be applied. We have comparatively evaluated pertinent methods for the, last, SR step of the proposed method [3], [4], [5], [27] and selected [27] because it yielded the relatively better results in terms of image quality, as well as, execution speed (see Sec. III-C). In other words, the proposed improvement stems from the registration stage that occurs in 3D (homography) instead of 2D (translation and rotation), while the proposed approach allows for employing the SR approach of choice.

III. EXPERIMENTS

The experiments targeted the evaluation of the proposed method in the following respects. First, the accuracy of homography-based registration was evaluated, in order to investigate if it is sufficient for applying SR. Second, the quality of the obtained SR images based on 2D registration and the proposed 3D registration is compared. Third, candidate SR methods were evaluated as to which one provides an image of better definition. In the experiments, we also compare the results of the evaluated SR methods to the magnification of the reference image (based on bicubic interpolation) to indicate the improvement in image quality over conventional image interpolation.

[1]http://www.opencv.org/

	Bicubic Interpolation	[27]	[29]	[30]	[31]
Time (s)	0.5	3252	18956	22265	6210

TABLE I

TIME (IN SECONDS) FOR PERFORMING SUPER RESOLUTION ON A 2912×2912 PIXELS IMAGE. BICUBIC INTERPOLATION WAS PERFORMED USING ONLY 1 IMAGE. THE REST, USING 9 IMAGES EACH.

All experiments were conducted on a conventional PC with an i7-4770 CPU, at $3.40\,GHz$ and $16\,GB$ of RAM. Computational time was dominated by application of the evaluated SR methods, while the duration of SURF feature matching and image registration was less than $1\,sec$. For the SR methods, their MATLAB implementation in [28] was utilized[2]. Execution times for the generation of a SR image with scaling factor 3 from 2912×2912 pixels are shown in Table I. Bicubic interpolation was performed using only 1 image, and [27], [29], [30], and [31], using 9 images each. Methods [6], [7] fall in the same category as they also use 2D registration to enable a SR resolution technique, as the above. We were unable to directly compare to these methods as they utilize a greater amount of images (in the order of 1 or 2 hundred), also acquired by a different modality.

Three datasets have been used in the experiments. To the best of our knowledge, a publicly available dataset of multiple retinal images from the same person, eye, and (approximate) time does not exist, hence we acquired three datasets for our experiments. For each dataset, images were obtained during a single session from the same eye of the same person, while no preprocessing has been applied. The first comprised of 9 fundus images acquired with a Nidek AFC-210 fundus camera. Image resolution is 2912×2912 pixels and Field of View (FOV) was $\approx 45^\circ$ in both dimensions. The second dataset contains 16 images obtained with a Heidelberg Flowmeter. The image resolution is 1536×1480 pixels and a FOV of $\approx 30^\circ$ in each dimension. The third dataset contains 16 images obtained with a fundus camera. Image resolution is 720×576 pixels and a FOV of $\approx 40^\circ$ in each dimension. The reference images for these two datasets are shown in Fig. 2.

The datasets are comprised of only a few images as the acquisition procedure, albeit non-invasive, if repeated induces fatigue to the eye, due to the bright illumination source that causes pupil contraction and in some cases lacrimation (secretion of tears) that prevent the further acquisition of fundus images.

A. Registration accuracy

To evaluate registration accuracy, we measured as registration error the distance of the corresponding points after registration. That is, for a homogeneous point $\mathbf{x}$ in a test image i ($i > 0$) its location in the reference image, after registration, is $H_i \cdot \mathbf{x}$. Let $\mathbf{x}'$ the matching point in the reference image. Then the measured error is $||\mathbf{x}' - H_i \cdot \mathbf{x}||$. The measured error

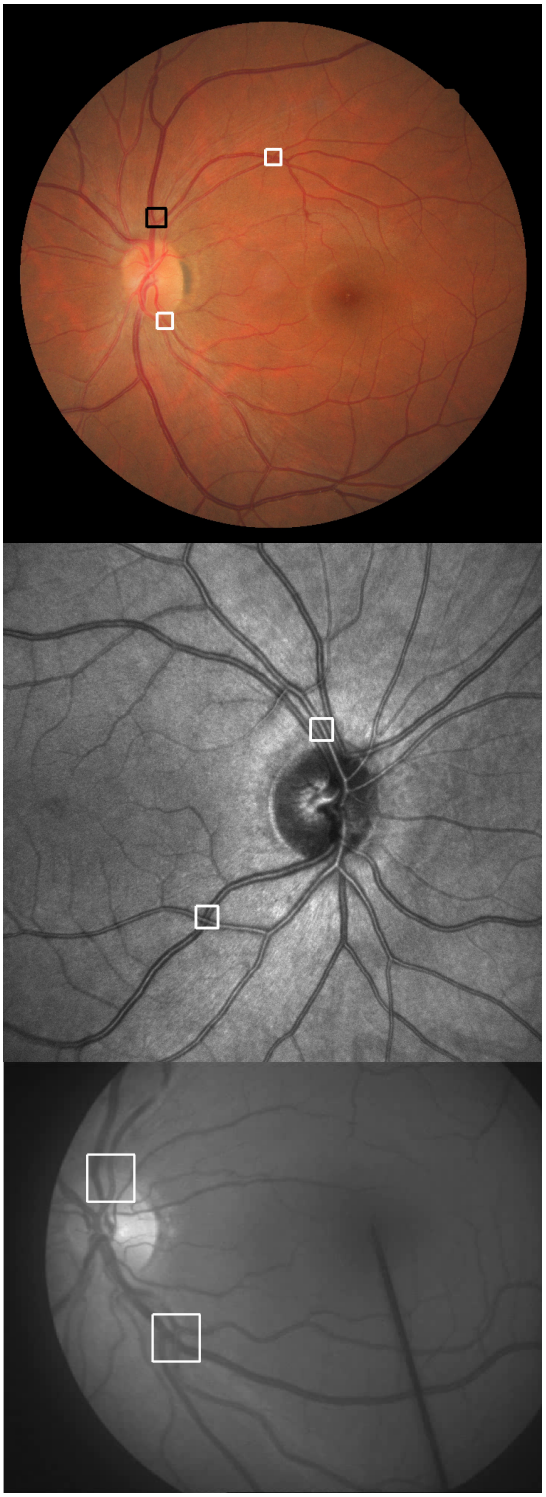

Fig. 2. Reference images for dataset 1 (top), 2 (middle) and 3 (bottom). Marked regions with solid white line correspond to the image details shown in Figs. 4, 5 and 6. The solid black line region in the top image corresponds to the image detail in Fig. 3.

[2]http://lcav.epfl.ch/software/superresolution

	Mean error	std	# matches
Dataset 1	0.4884	0.2451	81
Dataset 2	0.5851	0.2485	2621
Dataset 3	0.3875	0.2362	208

TABLE II

REGISTRATION ERROR AND STANDARD DEVIATION, IN PIXELS.

	This work	[4]	[5]	[3]	[32]
Dataset 1	11.6335	7.9317	0.5670	8.2380	9.1917
Dataset 2	9.5344	7.6581	5.9235	8.0751	7.3038
Dataset 3	17.0561	17.7945	11.3587	17.7945	17.7945

TABLE III

SNR (IN DB) OF SR RESULTS, FOR THE EXPERIMENT OF SEC. III-B.

bears the consequences of spurious keypoint matches which is, however, small due to the preliminary filtering in Sec. II.

It ought to be noted that if we were to use the 'SURF-established' correspondences for the above purpose, then error would be measured using the same correspondences that were used to estimate the homography. In that case, error computation would be biased. Hence independently established correspondences are employed and, in particular, correspondences established through SIFT features. As a verification, we ran the same experiment using SURF-established correspondences to observe about half the error (≈ 0.2 pixels), which we chose not to use in the evaluation. The obtained mean errors and standard deviation are reported in Table II, where it can observed that in this independently chosen control points, we obtain a subpixel accuracy in the registration. We, thereby, reason that registration accuracy enables the application of SR methods.

B. Comparison of registration methods

In this experiment, we compare the proposed registration method with other methods employed in the task of SR. The purpose of the experiment is to indicate the advantage of the proposed 3D, homography registration method over 2D registration methods that are conventionally employed in the task. Therefore we have employed the adopted SR method [27] and varied the registration approach. Two different experiments have been performed to quantitatively compare the registration methods.

1) Signal-to-Noise Ratio: In the first experiment, the Signal-to-Noise-Ratio (SNR) of the obtained images was calculated, using as reference the first image of each dataset. To indicate the role of the registration method more clearly, and restrict potential confounding of the result due to the combination of multiple images, only 4 images of the dataset have been utilized. Those images have been previously scaled with a scaling factor of 0.5. The SR scaling factor was 2 in all experiments, to generate a SR image of the same size as the original images. This scaling factor also casts the particular application of SR a square problem thereby avoiding potential improvement of the result due to the use of additional images. The purpose of this experiment is to generate a SR image of the same size as the original images, and to calculate the similarity between the SR image and the original image via the SNR. The proposed, in Sec. II, registration method was compared to [3], [4], [5] and [32]. In Fig. 3, the obtained results are compared in an image detail, clearly indicating that the proposed 3D registration approach has an advantage over 2D registration approaches in this problem.

Dataset 1	This work	[4]	[5]	[3]	[32]
Mean	0.4884	16.8608	447.9505	17.1637	15.2349
Std	0.2451	9.6545	384.3768	11.1891	7.7316

TABLE IV

REGISTRATION ERROR AND STANDARD DEVIATION, IN PIXELS, FOR 81 CONTROL POINTS IN DATASET 1

Given the nature of the images of some datasets, in which there are black frames that may bias the SNR calculation, a comparison omitting the black areas has been performed. The results (Table III) show that while in Dataset 3 (the one with the smallest images), our proposed registration method offers similar results as the existing ones, for Datasets 1 and 2 (where image sizes increases notably), our method outperforms the rest.

2) Pixel error: In the second approach for quantitative analysis, the independent control points calculated in Sec. III-A have been used for calculating the mean error and standard deviation of the 5 registration methods analyzed. The error distances have been calculated for control points in each image of the datasets. The results are reported in Tables IV, V and VI and show the registration error, as the mean 2D distance of the matched points after the registration with each evaluated method. The proposed registration, outperforms the other analyzed methods. In some cases, the increment in improvement is in the order of tens of pixels, indicating that the registration improvement is significant.

We note that the error, in the particular case of method [5], is much greater than the rest of the methods. In that method, the rotational component of registration was particularly erroneous, leading to very high inaccuracies at image periphery.

Dataset 2	This work	[4]	[5]	[3]	[32]
Mean	0.5851	52.2144	319.3092	15.5748	6.4975
Std	0.2485	35.3212	347.2220	25.7937	4.0704

TABLE V

REGISTRATION ERROR AND STANDARD DEVIATION, IN PIXELS, FOR 2621 CONTROL POINTS IN DATASET 2

Dataset 3	This work	[4]	[5]	[3]	[32]
Mean	0.3875	5.2442	96.9436	7.2677	5.1491
Std	0.2362	2.8381	60.3513	3.2337	3.2980

TABLE VI

REGISTRATION ERROR AND STANDARD DEVIATION, IN PIXELS, FOR 208 CONTROL POINTS IN DATASET 3

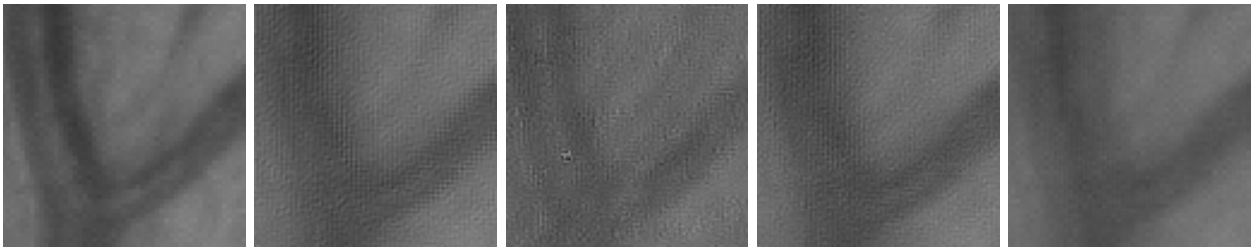

Fig. 3. Image registration comparison. SR 100×100 pixel image detail results (see Fig. 2), using [27], comparing the proposed 3D registration method to 2D registration methods. Showing the green channel to better show the results. Left to right: proposed method, [4], [5], [3] and [32].

C. Comparison of Super Resolution methods

In this experiment, we have registered images using the proposed registration approach and compared the output of the SR methods in [27], [29], [30], and [31]. The purpose of the experiment was to select the SR approach to be adopted by the proposed method. The comparison was performed by qualitative inspection of the images.

To evaluate the results, the SR methods were applied to the three sets of images. The experiment for dataset 1 was performed with $n = 3$ and $l = 9$ as parameters. For datasets 2 and 3, $n = 4$ and $l = 16$ were the parameters used. Indicative image details are shown in Figs. 4, 5 and 6. In the results, we also provide the bicubic interpolation of the reference image, by the same scaling factor, to indicate the contribution of the SR method in image quality. It is observed that the SR images exhibit less noise than both the original and the scaled ones and that vessels appear better defined.

Based on thorough inspection of the results, we have adopted the SR method [27] in the proposed approach. Nevertheless, we stress that the benefit of the proposed method stems from the, earlier, registration step. Thereby, the technique thereafter employed to generate the SR result can be substituted by more suitable according to imaging modality or number of available images.

IV. CONCLUSIONS

A method for SR in fundoscopy images has been proposed, which differs from existing approaches to retinal image SR by the fact that it considers the perspective differences between the combined images. To achieve this, a 3D registration method is employed, as a basis to combine multiple images, which does not require camera calibration.

In the experiments, we show that the proposed image registration method (a) provides subpixel accuracy and is, thus, suitable for application in the generation of SR images and (b) provides better image alignment than 2D registration methods that are conventionally employed in this task and, consequently, improve the quality of the obtained SR result. In some cases, the increment in improvement is in the order of tens of pixels, indicating that the registration improvement is significant. Moreover, the obtained image alignment provides a basis for the comparison of SR methods, which we utilize to select the best performing SR to employ in the context of this work. The obtained results provide better image resolution and definition and, thus, could potentially improve vessel segmentation and measurement in retinal images. Such an assessment is part of our future work.

Although that our results improve state-of-the-art in SR of retinal images, we acknowledge that there exists ample room for improvement. Our next step would be to account for the non-planar shape of the retinal surface during image registration. However, in that case, camera calibration would be required to accurately register images upon a non-planar 3D surface. Calibration of a fundus camera is a complex task, for the following reasons. First, the fundus camera contains several lenses, not just a single one. It also employs an auto-focus function not allowing for consistent image acquisition and, thereby, complicating calibration as multiple focal lengths need to be solved for. Furthermore, the specific fundus camera that we had access to does not allow for image acquisition unless it detects an eye in front of it; thus, specific equipment is required to perform the conventional grid-based calibration [33]. To overcome such issues, camera calibration could be estimated together with the shape of the imaged surface (retina), following the research avenue proposed in [10].

Another avenue of future work is to address the large computational time, albeit in MATLAB, required for the execution of SR. In this respect, we plan to capitalize of the inherent per-pixel potential of parallelizing the SR computation and utilize a programmable GPU approach to accelerate computation.

Finally, we note that the fact that arterial shape undergoes minor local changes due with heartbeat, is acknowledged. Our intention is to address this phenomenon, also, in our future work.

ACKNOWLEDGMENTS

Authors wish to thank Areti Triantafyllou and Panagiota Anyfanti, from the Hippokration General Hospital of Thessaloniki, Greece, for providing the images of the first dataset; Maged Habib from the Sunderland Eye Infirmary, United Kingdom, for providing the images of the second dataset; Toke Bek from Aarhus University, Denmark, for providing the images of the third dataset; Antonis A. Argyros for fruitful discussions; and the anonymous reviewers for their invaluable feedback.

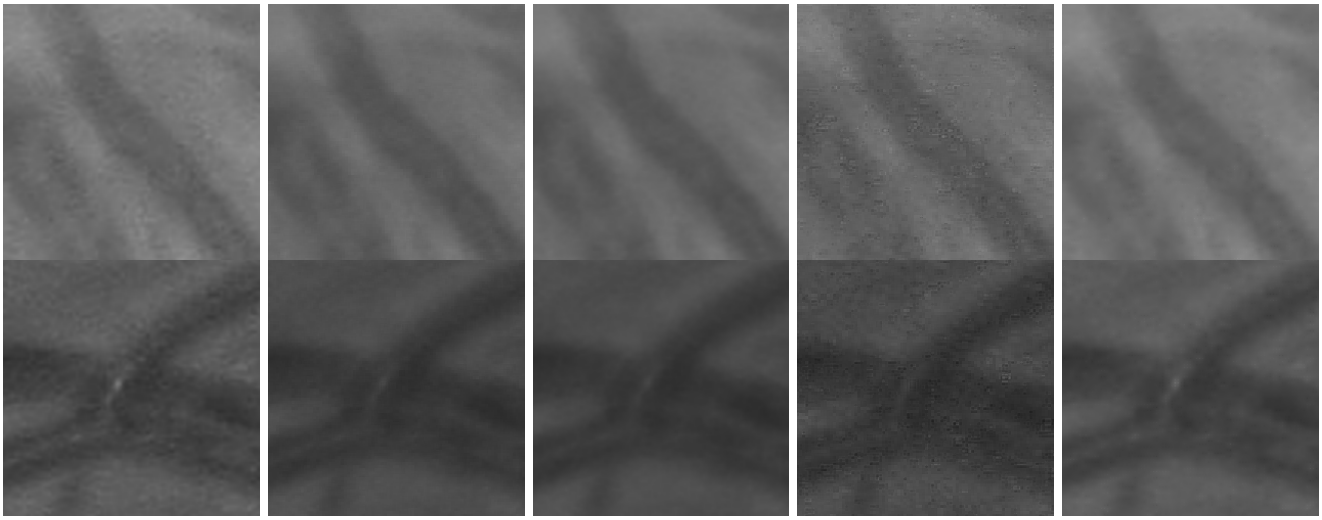

Fig. 4. Qualitative comparison of SR methods using the proposed registration for datasets 1, in two 250×250 pixel SR image details (see Fig. 2, top). Showing the green channel to better show the results. Left to right: bicubic interpolation, [27], [29], [30], and [31].

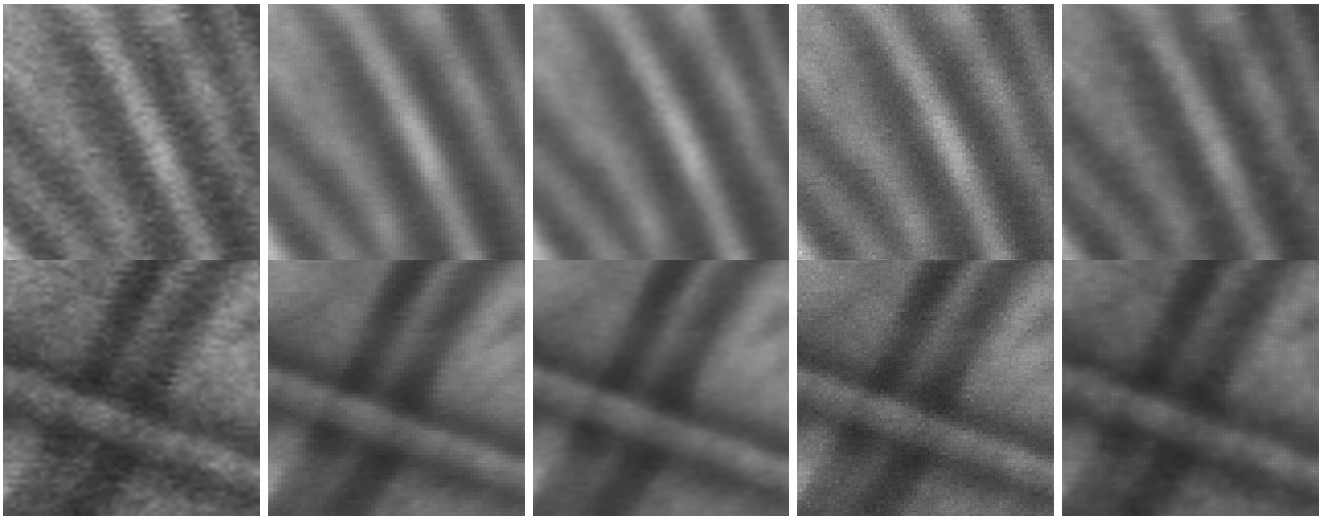

Fig. 5. Qualitative comparison of SR methods using the proposed registration for datasets 2, in two 250×250 pixel SR image details (see Fig. 2, middle). Left to right: bicubic interpolation, [27], [29], [30], and [31].

REFERENCES

[1] A. Grosso, F. Veglio, M. Porta, F. Grignolo, and T. Wong, "Hypertensive retinopathy revisited: some answers, more questions." *British Journal of Ophthalmology*, vol. 89, no. 12, pp. 1646–54, 2005.

[2] L. D. Hubbard, R. J. Brothers, W. N. King, L. X. Clegg, R. Klein, L. S. Cooper, A. R. Sharrett, M. D. Davis, and J. Cai, "Methods for evaluation of retinal microvascular abnormalities associated with hypertension/sclerosis in the atherosclerosis risk in communities study." *Ophthalmology*, vol. 106, pp. 2269–80, Dec 1999.

[3] P. Vandewalle, S. Süsstrunk, and M. Vetterli, "A Frequency Domain Approach to Registration of Aliased Images with Application to Super-Resolution," *EURASIP Journal on Applied Signal Processing*, vol. 2006, p. ID 71459, 2006.

[4] D. Keren, S. Peleg, and R. Brada, "Image sequence enhancement using sub-pixel displacement," in *Proceedings IEEE Conference on Computer Vision and Pattern Recognition*, 1988, pp. 742–746.

[5] L. Lucchese and G. M. Cortelazzo, "A noise-robust frequency domain technique for estimating planar roto-translations," in *IEEE Transactions on Signal Processing*, 2000, pp. 1769–1786.

[6] N. Meitav and E. N. Ribak, "Improving retinal image resolution with iterative weighted shift-and-add." *Journal of the Optical Society of America. A, Optics, image science, and vision*, vol. 28, no. 7, pp. 1395–402, Jul. 2011.

[7] G. Molodij, E. Ribak, M. Glanc, and G. Chenegros, "Enhancing retinal images by extracting structural information," *Optics Communications*, vol. 313, pp. 321–328, Feb. 2014.

[8] C. V. Stewart, C.-L. Tsai, and B. Roysam, "The dual-bootstrap iterative closest point algorithm with application to retinal image registration." *IEEE transactions on medical imaging*, vol. 22, no. 11, pp. 1379–94, Nov. 2003.

[9] C.-L. Tsai, C.-Y. Li, G. Yang, and K.-S. Lin, "The edge-driven dual-bootstrap iterative closest point algorithm for registration of multimodal fluorescein angiogram sequence." *IEEE transactions on medical imaging*, vol. 29, no. 3, pp. 636–49, Mar. 2010.

[10] Y. Lin and G. Medioni, "Retinal image registration from 2d to 3d," *IEEE Conference on Computer Vision and Pattern Recognition*, 2008.

[11] N. Ryan, C. Heneghan, and P. de Chazal, "Registration of digital retinal images using landmark correspondence by expectation maximization," *Image and Vision Computing*, vol. 22, no. 11, pp. 883–898, Sep. 2004.

[12] J. Chen, J. Tian, N. Lee, J. Zheng, R. T. Smith, and A. F. Laine, "A partial intensity invariant feature descriptor for multimodal retinal

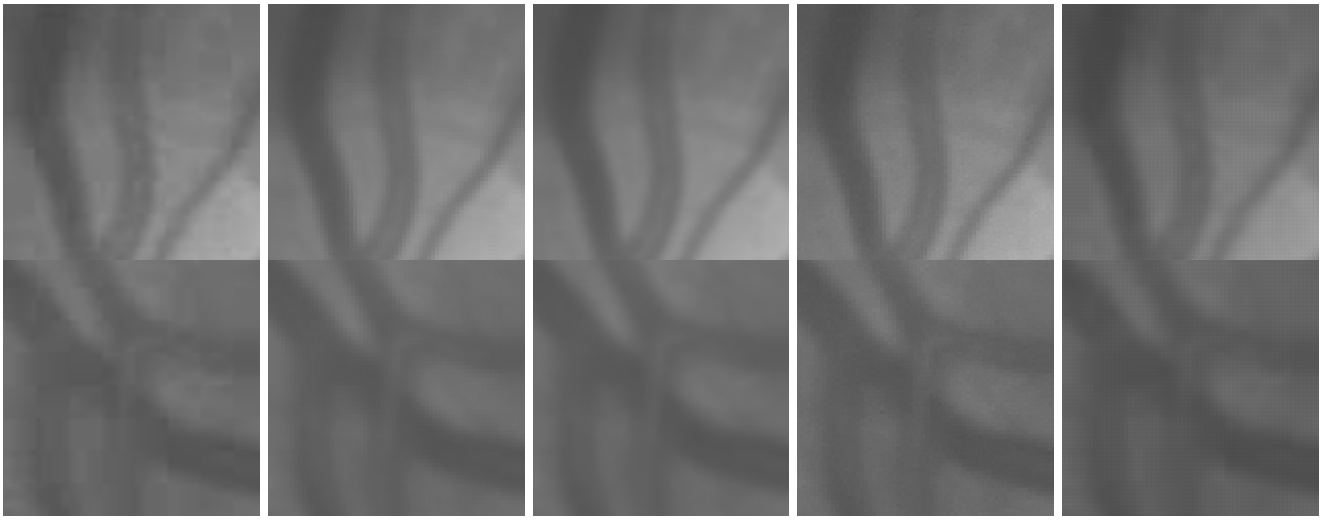

Fig. 6. Qualitative comparison of SR methods using the proposed registration for datasets 3, in two 250×250 pixel SR image details (see Fig. 2, bottom). Left to right: bicubic interpolation, [27], [29], [30], and [31].

image registration." *IEEE transactions on bio-medical engineering*, vol. 57, no. 7, pp. 1707–18, Jul. 2010.

[13] A. Perez-Rovira, R. Cabido, E. Trucco, S. Mckenna, and J. P. Hubschman, "RERBEE : Robust Efficient Registration via Bifurcations and Elongated Elements applied to retinal fluorescein angiogram sequences," *IEEE transactions on medical imaging*, vol. 31, no. August, pp. 1–11, 2011.

[14] J. Zheng, J. Tian, K. Deng, X. Dai, X. Zhang, and M. Xu, "Salient feature region: a new method for retinal image registration." *IEEE transactions on information technology in biomedicine*, vol. 15, no. 2, pp. 221–32, Mar. 2011.

[15] Y. B. Bathina, "Robust Registration of Retinal Images," Ph.D. dissertation, International Institute of Information Technology Hyderabad, 2013.

[16] C. Hsu and C. Lin, "Image super-resolution via feature-based affine transform," in *International Workshop on Multimedia Signal Processing*, Oct. 2011, pp. 1–5.

[17] P. Reel, L. Dooley, K. Wong, and A. Borner, "Multimodal retinal image registration using a fast principal component analysis hybrid-based similarity measure," *International Conference on Image Processing*, 2013.

[18] D. G. Lowe, "Distinctive image features from scale-invariant keypoints," *Int. J. Comput. Vision*, vol. 60, no. 2, pp. 91–110, Nov. 2004.

[19] O. Miksik and K. Mikolajczyk, "Evaluation of local detectors and descriptors for fast feature matching," in *International Conference on Pattern Recognition*, 2012, pp. 2681–2684.

[20] K. Mikolajczyk and C. Schmid, "A performance evaluation of local descriptors," *IEEE Trans. Pattern Anal. Mach. Intell.*, vol. 27, no. 10, pp. 1615–1630, 2005.

[21] H. Bay, A. Ess, T. Tuytelaars, and L. J. V. Gool, "Speeded-up robust features (surf)," *Computer Vision and Image Understanding*, vol. 110, no. 3, pp. 346–359, 2008.

[22] E. Oyallon and J. Rabin, "An analysis and implementation of the SURF method, and its comparison to SIFT," *Image Processing On Line*, pp. 1–31, 2013.

[23] M. A. Fischler and R. C. Bolles, "Random sample consensus: A paradigm for model fitting with applications to image analysis and automated cartography," *Commun. ACM*, vol. 24, no. 6, pp. 381–395, Jun. 1981.

[24] J. Nocedal and S. J. Wright, *Numerical Optimization*, 2nd ed. New York: Springer, 2006.

[25] S. Farsiu, M. D. Robinson, M. Elad, and P. Milanfar, "Fast and robust multiframe super resolution." *IEEE transactions on image processing : a publication of the IEEE Signal Processing Society*, vol. 13, no. 10, pp. 1327–44, Oct. 2004.

[26] S. Farsiu, D. Robinson, M. Elad, and P. Milanfar, "Fast and robust super-resolution," *IEEE Transactions onImage Processing*, vol. 13, pp. 1327–1344, 2003.

[27] M. Irani and S. Peleg, "Improving resolution by image registration," *CVGIP: Graphical models and image processing*, vol. 53, no. 3, pp. 231–239, 1991.

[28] P. Vandewalle, S. Süsstrunk, and M. Vetterli, "A frequency domain approach to registration of aliased images with application to super-resolution," *EURASIP Journal on Applied Signal Processing*, vol. 2006, pp. 1–14, March 2006. [Online]. Available: http://rr.epfl.ch/3/

[29] T. Q. Pham, L. J. van Vliet, and K. Schutte, "Robust fusion of irregularly sampled data using adaptive normalized convolution," *EURASIP Journal on Applied Signal Processing*, vol. 2006, pp. 1–17, 2006.

[30] P. Vandewalle, S. Susstrunk, and M. Vetterli, "Superresolution images reconstructed from aliased images," in *Proc. SPIE/IS&T Visual Communications and Image Processing Conference*, vol. 5150, 2003, pp. 1398–1405.

[31] A. Zomet, A. Rav-Acha, and S. Peleg, "Robust super-resolution," *Computer Vision and Pattern Recognition*, vol. 4, 2001.

[32] B. Marcel, M. Briot, and R. Murrieta, "Calcul de Translation et Rotation par la Transformation de Fourier, Traitement du Signal," *Calcul de Translation et Rotation par la Transformation de Fourier, Traitement du Signal,*, vol. 14, no. 2, pp. 135–149, 1997.

[33] Z. Zhang, "Flexible camera calibration by viewing a plane from unknown orientations," in *International Conference in Computer Vision*, 1999, pp. 666–673.